Effect of Agitation on Tin-Lead Alloy Deposition In a Methane Sulfonate System

C.S. Chen, C.C. Wan & Y.Y. Wang

Tin/lead alloy electrodeposition within methane sulfonic acid (MSA) solutions was studied. The thickness and composition of the deposit formed under static condition were investigated initially, then contrasted with the data obtained under a reflow system. It was found that when the electrolyte was stagnant, the high current area appeared on the edge region of the electrode surface where the lead deposition dominates, while the central region of the plate was the low current area that facilitated the tin deposition. Moreover, the increase of flow rate could significantly improve the distribution of Pb/Sn, although it had little effect on the composition of the deposition, which was mainly controlled by current density. Finally, the Pb/Sn alloy deposition in a MSA bath was found to be mainly controlled by the mass transfer of active ions. So the flow pattern and circulation greatly affect the current distribution of the alloy deposition. The flow pattern with a certain cell can be accurately simulated by mathematical modeling with the assistance of appropriate flow 3D software.

Tin-lead alloy plating is an important process for the electronics industry. One major traditional bath using fluoborate anions has met difficulty regarding its effluent treatment and is increasingly replaced with a methane sulfonate bath.[1-3] Relatively few papers have been published on this system's electrochemistry, however, either regarding its charge transfer kinetics or the deposition distribution as a result of mass transfer effect. Researchers here[4, 5] have studied the anodic dissolution of lead in methane sulfonic acid (MSA) by square-wave voltammetry and direct current polarography. They also studied the electrodeposition of tin-lead alloy on a rotating disk electrode and found that the reductions of tin and lead in MSA bath proceed in parallel without interaction.[6]

In this study, the aim was to gain more insight regarding deposit distribution and contribution in response to cell geometry and flow pattern. This information is understandably critical for precise control of the performance of this alloy plating system.

Experimental Procedure

The cell design is shown in Fig. 1. The anode used was 90/10 tin-lead alloy plate (0.09 x 0.12 x 0.003 m) and the cathode was pure copper plate (0.08 x 0.11 x 0.001 m) . The electrolyte was fed into the cell from the bottom in the x-direction and discharged from the top on the same side. The composition of the bath was similar to that used by Rosenstein:[7]

MSA 100 g/L, Pb^{+2} 2 g/L, Sn^{+2} 18 g/L, MH-1R (additive) 30 mL/L

Bath temperature was controlled at 25 ±0.2 °C. The polished electrodes were cleaned sequentially by deionized water, 20-percent sulfuric acid solution and 50-percent H_2O_2 solution.

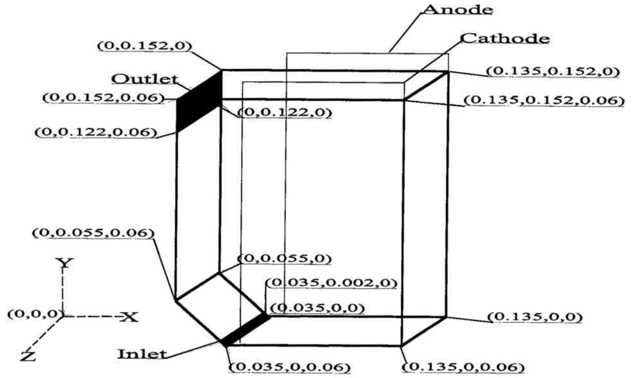

Fig. 1—Schematic diagram of the cell.

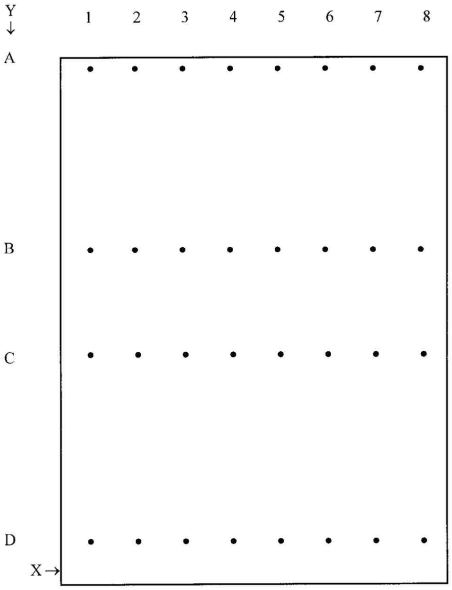

Fig. 2—The test positions of the cathode.

During plating, constant currents (1, 3, 6, 8 and 9 A/dm^2) were applied to the system for five min. Then the deposit thickness and composition at various locations on the cathode were measured by X-ray fluorescence (Fresh XDVM).

The positions of these test points on the cathode are shown in Fig. 2. There are eight points in the X-direction and four points in the Y-direction, so the uppermost left point can be designated as A1. After one run, the experiment was carried out with a different agitation rate to learn the effect of flow on the deposition.

Theoretical Considerations

The flow pattern within a cell is chiefly governed by the cell's geometry and agitation mode. Uniform distribution of deposits with respect to thickness and composition is a key criterion for the performance of a plating system. In most systems with fairly high current density, the distribution is mainly controlled by mass transfer effect, which is naturally directly related to the flow pattern near the cathode.

Accordingly, a simulation model was established to predict the flow pattern within the cell. The simulation result was

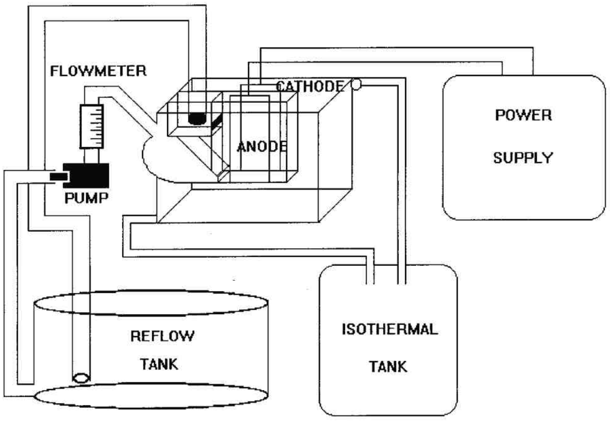

Fig. 3—Schematic flowchart of the apparatus.

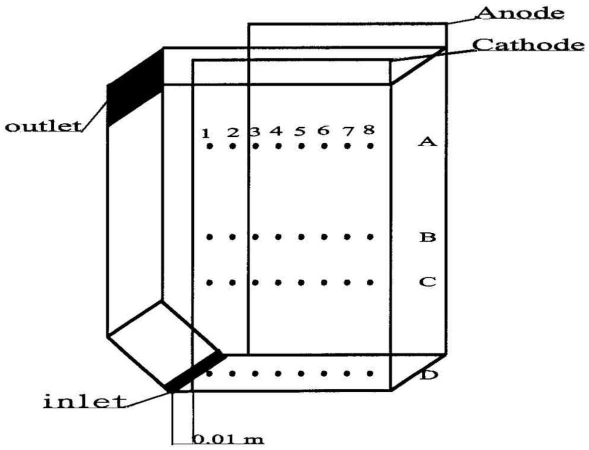

Fig. 4—Schematic positions of the plates in the reflux tank; cathode's measuring points shown by dots.

then compared with the metal distribution obtained from the experiments. The computation was based on software (cfx-flow 3D) developed by AEA Technology. The flow pattern within the cell was calculated by controlled volume and multiblock grid method,[8] as shown in Figs. 3 and 4.

In this study, agitation was achieved by a reflux flow pattern. The plating solution entered the cell from the left side of the bottom, flowed through the plating cell, and went out at the left side of the cell top. The governing hydrodynamic equations were numerically solved by the computer software. In the computation, the density and viscosity of the plating solution were assumed to be constant and were 1080 kg/m^3 and 0.0015 kg/msec, respectively. The boundary conditions were then as follows:

Inlet $u = Q_{IN}$, $v = 0$, and w = 0
Outlet $Q_{OUT} = Q_{IN}$
Free-Wall (Y = 0.126 m) $\tau_{YX} = 0$, and $\tau_{YZ} = 0$
Other walls $u = v = w = 0$

where τ_{YX} and τ_{YZ} are the viscous fluxes of X and Z-momentum in the Y-direction, Q_{IN} is the inlet flow quantity, Q_{OUT} is the outlet flow quantity, and u, v and w are the velocity components in the X, Y and Z directions, respectively.

The computation can be divided into three stages, namely preprocessing, solving, and post-processing. In the preprocessing stage, the appropriate grid mesh was set up. The cell was then divided into multi-blocks to speed up convergence and increase the accuracy. In this case, the cell was divided into four blocks. In the solving stage, the convergence criterion was set at 1 x 10^{-6} and it was also assumed that the flow is laminar, isothermal and incompressible.

In the post-processing stage, the size of the grid mesh was evaluated. It was found necessary to divide blocks 1 and 4 in the X, Y, and Z directions into 40, 6 and 20 divisions, respectively, and blocks 2 and 3 into 40, 20 and 20 divisions, respectively. Finer divisions did not lead to better results. The electrolyte flows very fast near the inlet in block 1 and also in areas near the cell's walls. The center region has the slowest flow. One noteworthy zone is at the right bottom corner where the flow was very slow. This is probably because the flow encountered a sharp rectangular corner, formed a dead-end and obstructed the smooth progression of the electrolyte.

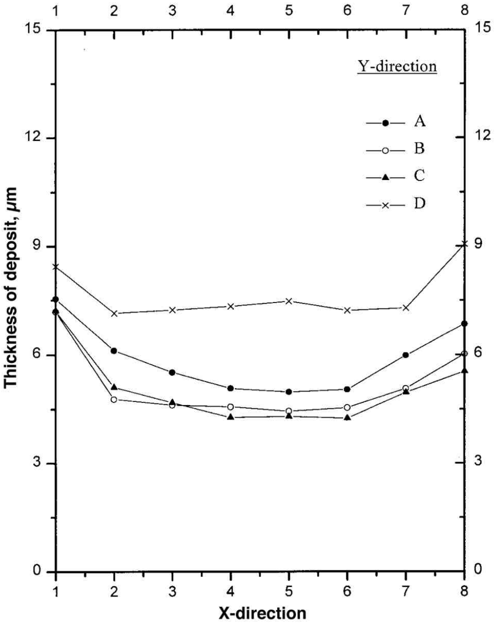

Fig. 5—Thickness distribution of deposit at 3 A/dm^2 without agitation.

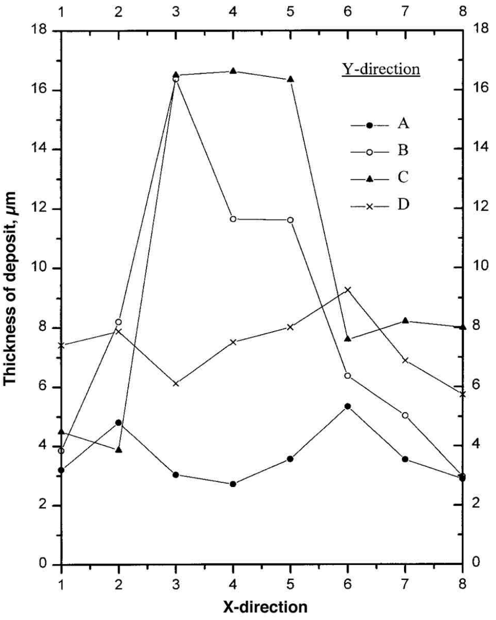

Fig. 6—Thickness distribution of deposit at 9 A/dm^2 without agitation.

The simulated flow pattern seems reasonable. It is sufficient to use a two-dimensional model in this case, but the model developed can be applied to a three-dimensional case. Its function to predict the flow pattern will become apparent in a more complex cell configuration.

Results & Discussion

Current Distribution & Composition Change In Unstirred Conditions

In a system without agitation, the deposition distribution on a cathode and the ratio of Pb/Sn are chiefly dependent on the geometry of the cell and the charge transfer kinetics. The result for typical Pb/Sn deposition in a MSA system is shown in Fig. 5, when the applied current was 3 A/dm^2. It is obvious that in the vertical direction, positions A and D possess a

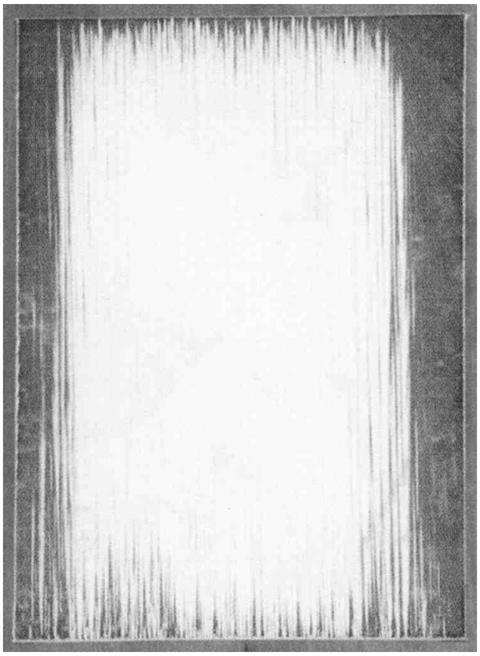

Fig. 7—Photo of deposit at 9 A/dm^2 without agitation.

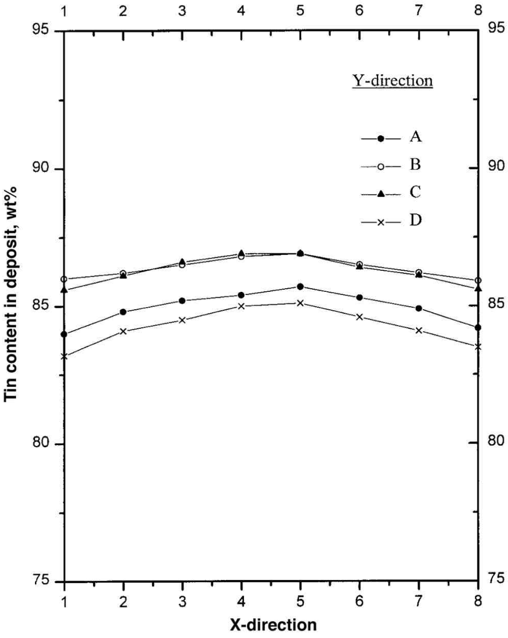

Fig. 8—Composition distribution of deposit at 6 A/dm^2 without agitation.

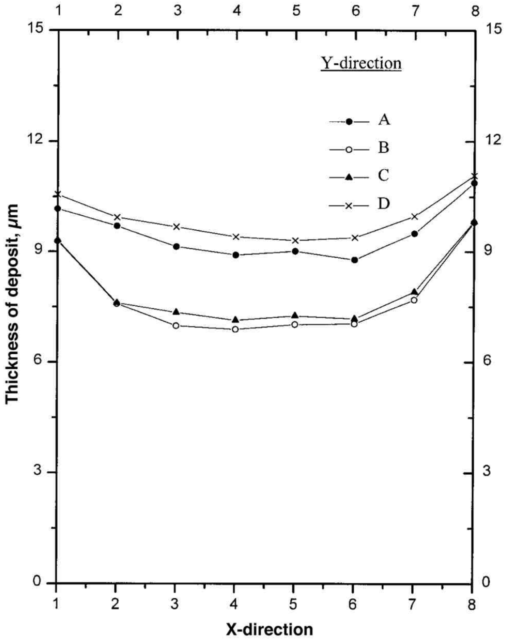

Fig. 9—Thickness distribution of deposit with inlet velocity of 0.0556 m/sec and 6 A/dm^2.

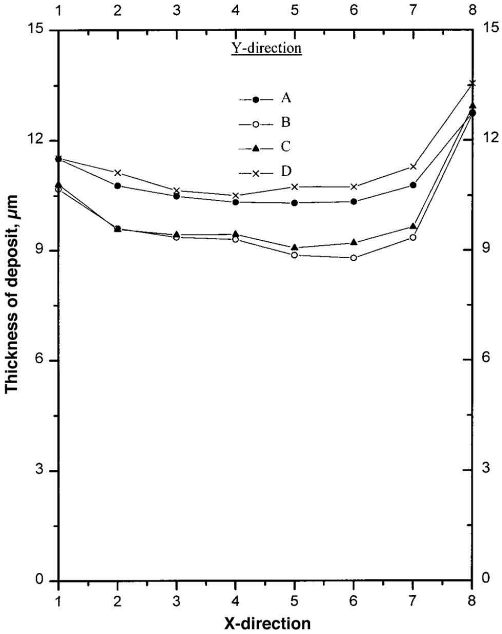

Fig. 10—Thickness distribution of deposit with inlet velocity of 0.1807 m/sec and 6 A/dm^2.

thicker deposit than positions B and C, which are in the middle section. Similarly, in the horizontal direction, positions 1 and 8, which are on the edge, show the highest current density. This edge effect is quite common for primary current distribution, and actually became more significant as the current was increased. This means the charge transfer resistance was relatively insignificant in this system, otherwise the secondary current distribution would be more uniform than the primary current distribution when the applied current was increased. In fact, Pletcher and Walsh also found a similar effect in their case.[9] They further found that if the current approached the limiting current, the distribution became more uniform. A similar result in our system is shown in Fig. 6, which shows a distribution pattern totally different from Fig. 5. This is because, in this case, the current density in the edge area approached the limiting value, so side reactions occurred and actual deposition was severely inhibited. Figure 7 is a picture of the deposit corresponding to Fig. 6. Apparently, the edge region shows distinct burnout.

Another important criterion regarding the performance of a Pb/Sn deposition system is the consistency of the Pb/Sn ratio in the deposit. Typical results are shown in Fig. 8, when the applied current was 6 A/dm^2. The variation of Pb/Sn is small with respect to either current or location. Still, a closer look shows a higher tin content existed in the central region and a larger current in general favored Pb deposition. This is reasonable, inasmuch as lead deposition in the MSA system has a higher exchange current density than tin deposition. Consequently, in lower current density regions, tin deposition is preferred.

Effect of Agitation

As mentioned previously, the charge transfer kinetics for a Pb/Sn/MSA system is rather fast, so the major controlling factor will be the flow rate and flow pattern, which directly influence the mass transfer of ions, especially in high current cases. Figure 9 shows the thickness distribution when the inlet flow rate is 0.0556 m/sec and the average current density is 6 A/dm^2. There was a significant improvement in thickness distribution when the inlet flow rate was increased from zero to 0.0556 m/sec. There was a thickness decrease in the edge area and a thickness increase in the central region in the latter case. If the flow rate was further increased to 0.0973 and 0. 1390 m/sec, the improvement trend continued. As the flow rate was increased, however, to 0.1807 m/sec, the overall improvement trend still existed, but the thickness at location 8 increased dramatically, as shown in Fig. 10. This means that the distribution is not necessarily more uniform if circulation is indefinitely increased. In this particular case, if the plating rack can be designed to avoid location 8, then fast and uniform plating results with sufficient circulation.

The Pb/Sn ratio in the deposit must also be precisely controlled in the electronics industry. For instance, for IC lead-frame manufacturing, the common requirement for tin content is from 80 to 95 wt pct. In production, various methods, including a dummy anode or shield, were employed

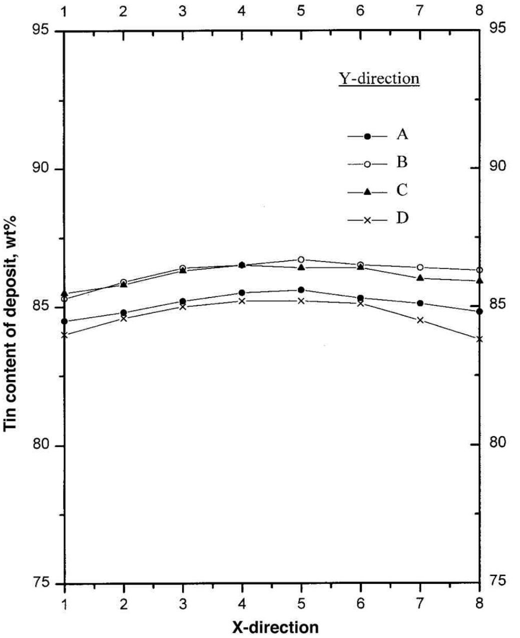

Fig. 11—Composition distribution of deposition with inlet velocity of 0.1390 m/sec and 6 A/dm^2.

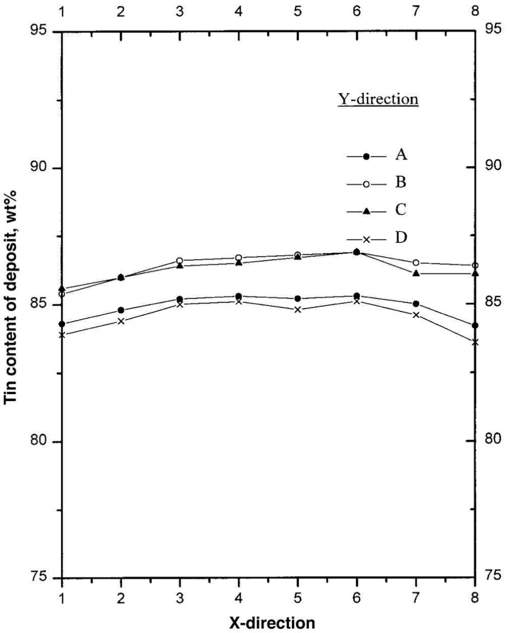

Fig. 12—Composition distribution of deposit with inlet velocity of 0.1807 m/sec and 6 A/dm^2.

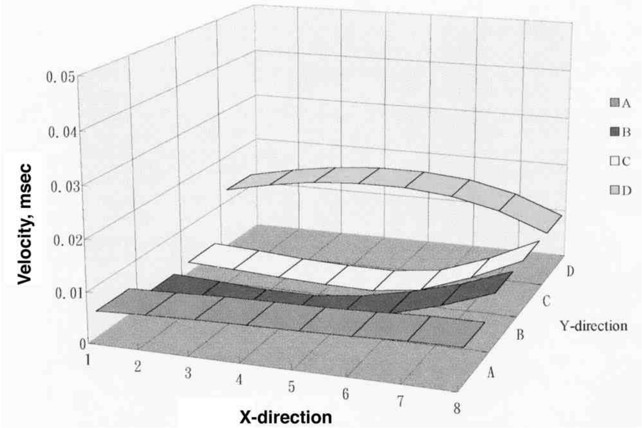

Fig. 13—Velocity simulation of plating tank with inlet velocity of 0.0556 m/sec and Z-coordinate at 0.03 m, where simulation positions correspond with measuring points.

to control the current distribution and composition consistency.[11] Very few publications address the effect of circulation on composition consistency. The result in this respect is shown in Figs. 11 and 12, where the flow rate was controlled at 0.1390 and 0.1807 m/sec, respectively. A comparison of Figs. 8 and 11 shows that the alloy composition changed very little with agitation. For instance, at locations D1 and D8, the tin content was 83.2 and 83.5 wt pct in Fig. 8 and 83.5 and 83.3 wt pct in Fig. 11.

Correlation of Simulation & Experiment

The major purpose of model simulation is naturally to reduce the amount of experiment. Figure 13 shows the simulated flow distribution when the inlet flow rate was set at 0.0556 m/sec. Apparently, in the Y-direction, the D-region shows the highest flow rate, with the A-region coming next. The flow in the B or C region increases rapidly, however, when it approaches the edge in the X-direction. This flow distribution matches well with the thickness distribution shown in Fig. 9.

A similar match can also be found when the circulation rate was increased to 0.0973 and 0.1390 m/sec. Thus it implies that the system is basically mass-transfer controlled and that our model simulation can accurately predict the flow pattern that directly influences the mass transfer.

Findings

1. The Pb/Sn alloy deposition in a MSA bath was found to be mainly controlled by the mass transfer of active ions. The flow pattern and circulation then greatly affect the current distribution of the alloy deposition.
2. The flow pattern within a certain cell can be accurately simulated by mathematical modeling with the assistance of cfx-flow 3D software.
3. Increase of flow rate could significantly improve the distribution of Pb/Sn distribution, although it had little effect on the composition of the deposit, which was mainly controlled by current density.

Editor's note: *Manuscript received, September 1998; revision received, December 1998.*

References

1. W.A. Proell, *Ind. Eng. Chem.*, **40**, 1129 (1948).
2. L. Deresh, *Metal Finishing*, **88**, 23 (1990).
3. M.I. Smimov, K.M.Tyutina & A.N. Popov, *Russion J. Electrochem.*, **31,** 498 (1995).
4. W.L. Hsueh & C.C. Wan, *J. Chin. I. Ch. E.*, **20,** 43 (1989).
5. W.L. Hsueh & C.C.Wan, *Bull. Electrochem.*, **6,** 790 (1990).
6. C.S. Chen, C.C. Wan & Y.Y. Wang, *Trans. Inst. Met. Fin.*, **76,** 54 (1998).
7. C. Rosenstein, *Metal Fin.*, **88,** 17 (1990).
8. CFDS, CFX-F3D Version 4.1 User Manual, Computational Fluid Dynamic Services, AEA Industrial, Harwell Laboratory, Oxfordshire, U.K., 1995.
9. D. Pletcher & F.C. Walsh, *Industrial Electrochemistry,* 2nd ed., Blackie Academic & Professional, London, 1990; p. 120.
10. T. Sonoda, H. Nawafune & S. Mizumoto, *Plat. and Surf. Fin.*, **82,** 66 (March 1995).
11. M. Jordan, *The Electrodeposition of Tin and Its Alloys,* E.G. Leuze, Germany, 1992; p. 284.

About the Authors

C.S. Chen is a doctoral candidate in the Department of Chemical Engineering, National Tsing-Hua University, Taiwan. His research activities include direct alloy plating and related fields. He obtained his MS from the same university.

Chi-Chao Wan is a professor in the Department of Chemical Engineering, National Tsing Hua University, Hsinchu, Taiwan, R.O.C. Dr. Wan is a past president of the AESF Taipei Branch, and his major research interest is in surface treatments for the printed circuit board industry, as well as plating, electrochemistry and metal finishing. He holds a DSc degree from Columbia University.*

Y.Y. Wang is a professor in the Department of Chemical Engineering, National Tsing-Hua University (NTHU). He holds an MS from NTHU and undertakes research in electroplating and battery systems.

** To whom correspondence should be addressed.*